Wear Behaviour of SLS WC-Co Composites

S. Kumar, [a,1] J.-P. Kruth [b] L. Froyen [c]

[a] *Dept. of Mechanical and Aerospace Engineering, Utah State University, USA*

[b] *Dept. of Mechanical Engineering, Katholieke Universiteit Leuven, Belgium*

[c] *Dept. of Metallurgy and Materials Engineering, Katholieke Universiteit Leuven, Belgium*

Reviewed, accepted September 10, 2008

Abstract

Selective Laser Sintering (SLS) is used not only for processing polymers, metals and ceramics but also composites. The present paper deals with the processing of WC-Co composites with and without Cu and gives light on its properties after bronze infiltration. Evaluation of wear resistance of WC-Co-based composite is important for its various applications. The wear properties shown by the composites have been determined using fretting wear tests, and described along with their microstructures.

Key words: : Selective Laser Sintering (SLS), WC-Co-Cu, Fretting wear

1 Introduction

Composites are needed when individual materials fail to yield adequate properties. By judicious choice of various components, composites are made to offer tailored properties.

In SLS, composites have been manufactured mainly by using three methods: 1) by taking materials or materials mixtures similar to that of an end product [1], e.g. formation of a WC-Co composite from a powder mixture of WC and Co [2,3], 2) by using an in-situ reaction, e.g. formation of Cu-TiC-TiB

[1] corresponding author. Address: Dr. Sanjay Kumar, Department of Mechanical and Aerospace Engineering, Utah State University, 4130 Old Main Hill, Logan, Utah 84322, USA Tel: +1 435 797 1803, Fax: +1 435 797 2417, Email: sanjay.kumar@usu.edu

25 August 2008

composite from a powder mixture of Cu-Ti-B_4C [4], 3) by using furnace treatment, e.g. formation of Al/AlN composites by post-processing in an oven in the presence of nitrogen gas and an infiltrant Al alloy [5].

The formation of composite of tungsten carbide ceramic and cobalt metal is preferred over other cermet composites because:

(1) Cobalt has a high melting point (1493°C) and high temperature strength,
(2) It forms a liquid phase with WC at 1275°C and forms eutectic which dissolves 10% WC. The dissolved WC reprecipitates on solidification giving strength and,
(3) WC does not dissolve Co which allows a small amount of Co to be required as a binder.

Other binders which could be used are Ni, Fe and other metallic alloys.

The SLS of WC and Co has been inspired from their widely acknowledged properties obtained using conventional sintering techniques. Work has been done to make WC-Co composite using SLS followed by Cu infiltration [6–8]. Major work was done at KU Leuven where successful injection mould products from WC-9 wt.% Co were made using SLS followed by copper infiltration [2]. The mechanical properties achieved were comparable to that of a tool steel [9].

The present work deals with the formation of WC-Co composites using a SLS machine. Various compositions of WC and Co has been laser sintered and infiltrated with bronze. Their wear behaviour has been characterized using fretting wear tests.

The research work as shown in the paper has been conducted in two successive stages: preliminary experiment and final experiment. Preliminary experiment is meant to find right compositions and parameters for processing while the final experiment is done to build parts with few selected composition and parameters. The results obtained from these two sets of experiments are presented separately.

2 Experiments

2.1 Machine

The machine used for research was an enhanced 100 W DTM Sinterstation 2000, originally built for processing polymer powders for RP purposes or for processing powders containing a significant amount of polymer for RT purposes using a 50 W CO_2 laser. The original machine was not suitable for

processing high-melting point powders such as ceramic and metals because of its limited laser power. The original machine also needed large amount of powders as the built area was large requiring much powders for each new layer deposition.

The machine was modified to overcome its limitations by equipping it with a laser of 100 W power enhancing its melting capacity and an insert of 90 mm diameter for reducing the built area.

2.2 Preliminary Experiments

2.2.1 Materials

In a first series of experiments, 9% and 50% Co of size less than 37 μm of irregular shape is mixed with WC of size less than 45 μm of prismatic shape. This powder is laser sintered and infiltrated with bronze. As it is essential to infiltrate the laser sintered samples, tests were also done with a mixture of WC and Co powders premixed with an infiltrant material such as Cu before SLS. The composition taken in that case is WC with 12 %Co and 18 % Cu. Co is of size less than 37μm and of spherical shape, while Cu is spherical powder produced by gas atomization of size from 40 to 63μm. The WC powder is the same as mentioned earlier.

2.2.2 Experimental Parameters and Processing

Experiments were done with a modified DTM Sinterstation 2000 having a CO_2 laser of 100 W nominal power. The maximum laser power available at that time was 80 W and the laser spot size was 590μm. The changeable experimental parameters are scan spacing, layer thickness and laser power. Scan spacing was kept constant at 0.1 mm.

The experimental parameters for WC-18Cu-12Co and WC-50Co are the same, i.e. layer thickness of 0.3 mm and laser power of 40 W. WC-9Co is laser sintered using two sets of parameters: (1) layer thickness 0.5 mm and laser power 50 W and, (2) layer thickness 0.3 mm and laser power 25 W. The second set of parameters was chosen to make the samples more porous in order to maximize the benefit of infiltration. All samples were infiltrated with bronze comprising 10% Sn.

A 25 hrs furnace treatment cycle was programmed to maintain a temperature of 1050°C for 5 hrs allowing the bronze to melt and to infiltrate the part. The oven then cools down to a temperature below 200°C while a flow of nitrogen and hydrogen is maintained to avoid oxidation (reduction by hydrogen). The

diagram for the temperature cycle is given in the Figure 1.

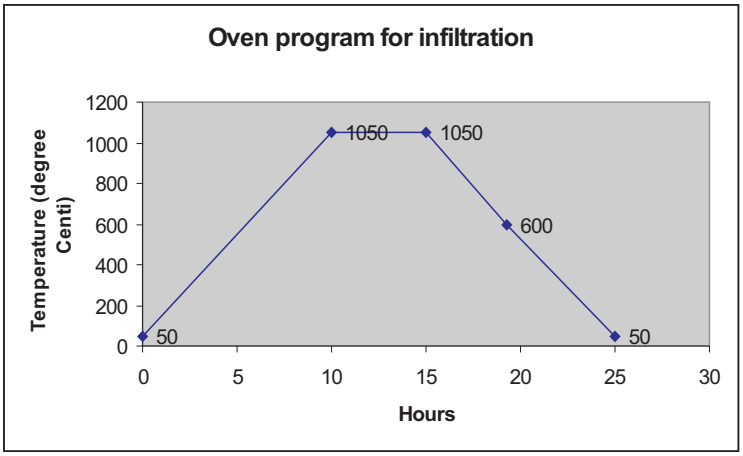

Fig. 1. Temperature-time diagram for infiltration

The weight of bronze needed for infiltrating a sintered sample is determined by estimating the porosity of the sample (by density measurement). This weight amount of bronze particles is then put in contact with (on top of) the porous green part to guarantee infiltration through capillary action once melting occurs in the furnace. The samples and the bronze are covered by alumina powder for homogeneous heat transfer and infiltration.

2.3 Final Experiments

2.3.1 Materials and Experimental Parameters

Materials taken for investigation were WC-9Co and WC-12Co. The sizes of WC particles (prismatic shape) were from 44 to 77μm while Co particles (irregular shape) were less than 37μm.

The selected parameters which gave the best properties are given in Table 1. WC-12Co has been laser sintered with both 40 and 50 W while WC-9Co has been sintered only with 80 W as shown in Table 1. The laser sintered parts were again infiltrated with bronze.

2.4 Fretting Wear Test

Fretting is a wear phenomenon occurring when two contacting solids are subjected to a relatively oscillatory tangential motion of small displacement amplitude [10]. Fretting can be applied by (1) keeping the counterbody fixed and linearly vibrating the specimen, (2) keeping the specimen fixed and linearly

Materials	Laser Power (W)	Height (mm)	Layer Thickness (mm)
WC-12Co	80	0	0.1
	40	0.2	0.3
WC-12Co	80	0	0.1
	50	0.2	0.3
WC-9Co	80	0	0.1
	80	1	0.2

Table 1
Experimental parameters for final experiments

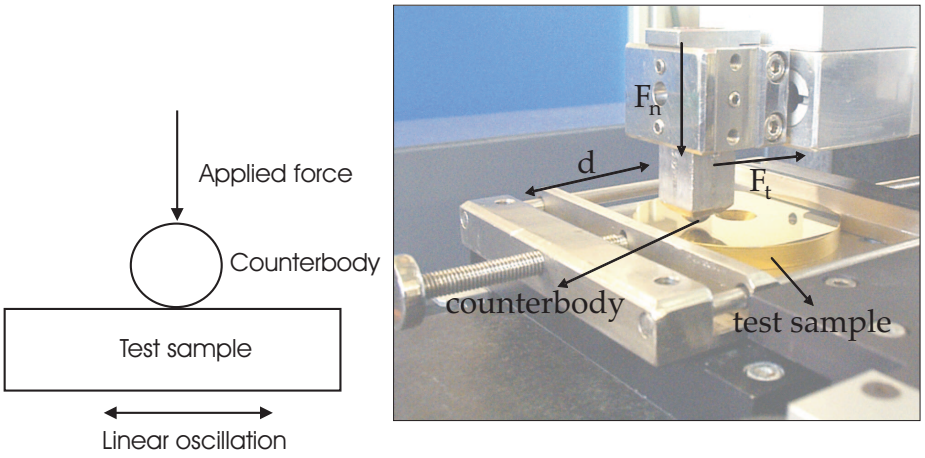

Fig. 2. Schematic diagram of the fretting test (left diagram) and the fretting test setting (right photograph)

vibrating the counterbody. In the present case, type 1 has been adopted. The specimen is mounted on a translation table which can be oscillated by a stepping motor. The displacement of the specimen is measured by an inductive displacement transducer and the friction force is measured with a piezoelectric transducer. The friction coefficient and total dissipated energy are calculated from the on-line measured tangential force [11]. A schematic diagram of a fretting test and part of a fretting apparatus is given in Figure 2.

Experimental parameters were selected in such a way that all tests could be executed under elastic contact conditions. A chrome steel ball of 30 mm was selected as counterbody. The parameters for the tests were as follows: Applied load- 2, 4, 6 N, Sliding distance (amplitude)- 200 μm, Frequency- 10 Hz, No. of cycles- 2000, 5000 and 10000, Temperature- 25°C and Humidity- 52%.

3 Results and Discussions

3.1 Results obtained from Preliminary Experiments

The infiltrated samples were characterized for their hardness and strength. Mainly, Brinell hardness was measured which was later converted into Rockwell B hardness for comparison with earlier measured samples. Bending strength were determined for some selected samples. The test methods and instruments were the same as described elsewhere [12]. Besides mechanical properties, their compositions in weight percent were also determined using XRF. The values are given in Table 2. The table does not show the amount of pores obtained for each type. Nevertheless, from the value of corresponding hardness, it could be assessed. It shows that WC-9Co/Bronze processed with low laser power has lowest porosity while the same that processed with high laser power furnishes highest porosity.

Powder mixture/ infiltrant	Final composition (in wt.%) excluding porosity	Hardness (HB)
WC-18Cu-12Co/Bronze	WC-56, Co-6 Cu-37, Sn-1	53
WC-9Co/Bronze	WC-66, Co-5 Cu-25, Sn-4	26
WC-9Co/Bronze (Low laser power)	WC-31, Co-3 Cu-60, Sn-6	155
WC-50Co/Bronze	WC-22, Co-22 Cu-50, Sn- 6	84

Table 2
Material composition and hardness of infiltrated laser sintered samples (from pre experiments)

In case of WC-9Co processed with higher laser power (50 W) while using a thicker layer thickness of 0.5 mm, the high laser power not only caused melting of the binder and closing of the pores (which prevented total infiltration) but also bigger pores resulted which were too big to be filled by capillary action. This resulted in low hardness. Figure 3 shows SEM micrographs of infiltrated WC-9Co samples processed with low and high laser power respectively. In the micrograph, grey prismatic zone shows WC, smaller grey areas are Co, dark areas are infiltrated bronze and darkest black areas are pores. Micrographs show that Co is scarce while WC is surrounded by bronze implying that in

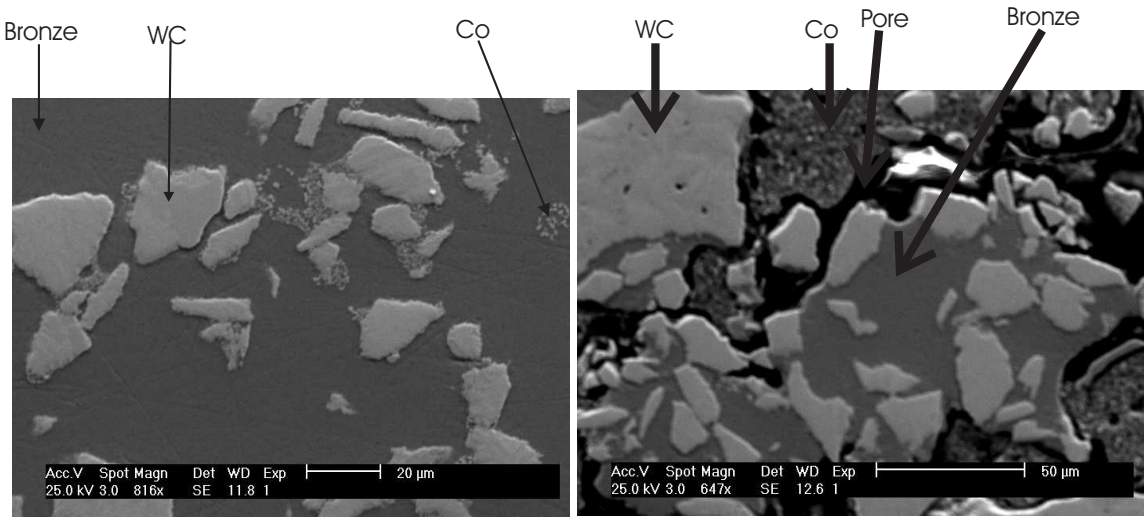

Fig. 3. SEM micrographs of infiltrated WC-9Co samples processed with low and high laser power respectively (from pre experiments)

an SLS sample, many WC were stacked in the sintered structure instead of getting bonded by Co. Micrograph corresponding to that of high laser power shows higher porosity directly resulting into a lower hardness.

WC-9Co processed with higher laser power gives the lowest hardness but it contains a higher amount of WC than that processed with low laser power (25 W) as shown by its composition in Table 2.

The final composition of an infiltrated WC-18Cu-12Co sample contains relatively a higher amount WC than that of WC-50Co. For WC-18Cu-12Co (70 % WC) the final part contains 56 % WC (a reduction to 80 % of the initial 70 % WC). For WC-50Co (50 % WC) the final part contains 22 % WC (a reduction to 44 % of the initial 50 % WC). In the later case, supplied laser energy is not sufficient to melt all binders resulting in a more porous product.

The hardness shown by WC-9Co processed at higher laser power is even less than that by WC-18Cu-12Co demonstrating that higher laser power combined with a small amount of binding element is not a good option for obtaining better results.

3.1.1 Results from Wear Tests

In order to verify that elastic contact condition exists between counterbody and sample during fretting test, tangential forces versus displacement graph has been observed for their rectangularity after some cycles [13]. The graphs for WC-9Co (low laser power type) and WC-50Co are shown in Figure 4 as noted after 9000 cycles for the highest experimental applied load, i.e. 4 N. The graph is almost rectangular in case of WC-9Co while fully rectangular for

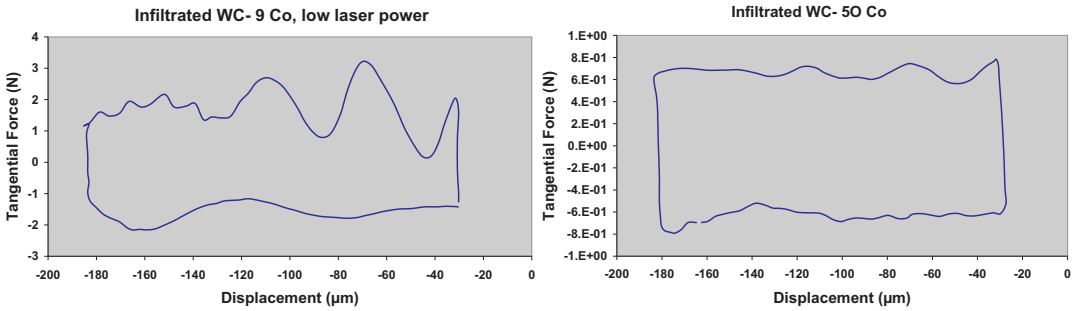

Fig. 4. Tangential force-Displacement curves for WC-9Co and WC-50Co after 9000 cycles for 4 N load (from pre experiments)

WC-50Co showing that only wear type condition occurs during fretting.

Wear volumes obtained after fretting tests are given in Table 3 alongwith results obtained from other commercial materials tested at the same conditions.

Wear volumes for WC-18Cu-12Co at both applied loads are exceedingly high (see Table 3) and the material also shows lower hardness and strength (see Table 2) implying that this product is not suitable as a wear-resistant material or for any applications requiring strength. The high wear rate could be due to the presence of pores in the sample.

WC-9Co (low laser power type) furnished the highest hardness and it is interesting to observe its wear behavior. At a low load of 2N, it demonstrates comparable wear resistance to one commercial wear resistant material, LaserForm, and performs better than the other SLS material, DirectSteel. But at a higher load of 4N, it gives enormous high wear as shown in Table 3. The reason could be attributed to the lack of hard component (WC) in sufficient amount in the infiltrated WC-9Co combined with pull-out of WC particles during fretting. It brings to the attention that being hard and dense is not sufficient to be wear resistant: it is not sufficient to produce a pore-free product with hard inclusions but also to manage to retain hard components in the product for wear applications.

The Coefficient of Friction (COF) obtained for WC-9Co (low laser power type) alongwith other comparable materials have been given in Table 4. It shows that the COF for all the materials are high and need to be improved for better performance.

3.2 Results obtained from Final Experiments

The density of the samples were measured according to Archimedes' principle while Brinell hardness tests and bending tests were done to determine their hardness and strength.

Materials	Applied Load (N)	Wear Volume ($10^3\mu$m)
WC-18Cu-12Co	2	4438
	4	5963
WC-9Co (low laser)	2	12.7
	4	1242
WC-50Co	4	4167
LaserForm	2	10.7
	4	30
DirectSteel	2	54
	4	83
WC-9Co/Cu(old [9])	2	1.1

Table 3
Wear volumes after fretting tests (from pre experiments)

Materials	Applied Load (N)	COF
WC-9Co (low laser)	2	0.73
	4	0.65
LaserForm	2	0.7
	4	0.7
DirectSteel	2	0.85
	4	0.7
WC-9Co/Cu(old [9])	2	1

Table 4
Coefficient of Friction (COF) after fretting tests (from pre experiments)

The density of the present samples alongwith that of samples made by an earlier researcher [9] are given in Table 5. The table shows that in case of WC-12Co, the one processed with high laser power gave higher density before infiltration (green density) but lower density after infiltration, showing that the supply of higher laser energy melted more binder material and closed the pores which prevented the infiltration to take place smoothly resulting in a lower final density.

However, WC-9Co processed with highest laser power gave a higher green density as well as a higher final density, showing that in this case the amount of binder material was not enough to hamper infiltration. The final density reached is 96%.

The density of WC-9Co is the highest as shown in Table 5.

Materials	% Green Density	% Final Density
WC-12Co	44	92
WC-12Co (high laser power)	58	76
WC-9Co	63	96
WC-9Co (old [9])	43	95

Table 5
Density of laser sintered samples with and without infiltration (from final experiments)

The hardness and bending strength measured for the infiltrated samples are given in Table 6. The Brinell hardness measured for WC-12Co/Bronze and WC-9Co/Bronze was 150 and 242 HB, respectively. These values are converted to Rockwell B hardness 85 and 103 HRB, respectively for ease of comparison with other values. The table shows that WC-9Co gives more hardness and strength than WC-12Co and is comparable to the properties shown by tool steel.

Materials	Hardness (HRB)	Strength (MPa)
WC-12Co/Bronze	85	596
WC-9Co/Bronze	103	714
WC-9Co/Cu (old [9])	81	418
Tool steel 1.2312	108	800

Table 6
Hardness and bending strength of samples (from final experiments)

On comparing the hardness value for WC-9Co/Bronze using Table 2 and Table 6, it is clear that SLS parameters play a vital role in determining the final hardness of the samples. Table 2 shows that using a combination of laser power and layer thickness of 50 W and 0.5 mm gave hardness of 25 HB while 25 W and 0.3 mm gave 155 HB. It is because in the first case of 25 HB, the particular combination of SLS parameters gave rise to melting and creation of scaffold which prevented infiltration resulting into lower hardness. The dominant reason for lack of infiltration was loss of capillary effect. In the second case of 155 HB, it was the absence of such high amount of melting and scaffold as observed in the first case which led to an increase in hardness of 155 HB. Table 6 shows an achievement of high hardness of 103 HRB (242 HB) for the same composition using SLS parameters of 80 W (laser power) and 0.2 mm (layer thickness). It was because of the complete absence of scaffold leading to relative high green density, suitable for infiltration. The formation of

closed pores due to melting prevented further infiltration and further increase of hardness. Therefore, the final density achieved was 96% in place of 100 %.

3.2.1 Results from Wear Tests

Surfaces were prepared by fine polishing to 1 μm. Besides, other samples cut by wire-EDM cutting were also used for wear testing. The effect of surface roughness resulting from EDM cutting on total wear volume was minimized by using a higher number of cycles (10000) for fretting so that the wear rate obtained will correspond to surface strength minus surface roughness effect. In some cases, small numbers of cycles (2000, 5000) were used to verify the anomaly found in the initial part of the COF versus no. of cycles curves obtained after 10000 cycles.

Coefficient of Frictions (COFs) against No. of cycles were drawn for infiltrated WC-12Co and WC-9Co samples at both surface conditions (EDM cut and diamond polished) for various applied loads. COF found for some last cycles for 10000 cycle tests are denoted as 'Final COF' and are given in Table 7 for various conditions.

Infiltrated materials	Surface	Applied load (N)	Final COF
WC-12Co	EDM	2	0.1
	EDM	4	0.15
	EDM	6	0.25
	EDM	9	0.55
WC-9Co	EDM	2	0.25
	EDM	4	0.7
	EDM	6	0.75
WC-12Co	polished	2	0.7
	polished	4	0.45
WC-9Co	polished	2	0.65
	polished	4	0.4

Table 7
Final COF of infiltrated samples after wire-EDM cutting or diamond polishing (from final experiments)

The table shows that for EDM cut surfaces, at a low load of 2N, both materials give very good COF (0.1 and 0.25 for WC-12Co and WC-9Co, respectively). But at higher load their COFs increase showing that an increased load has brought a change in the surface condition either of sample or counterbody, or

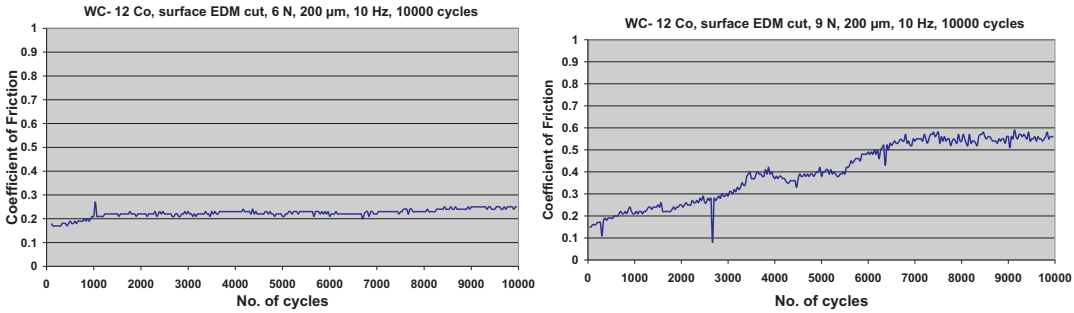

Fig. 5. COF vs No. of Cycles obtained for EDM cut surface of infiltrated WC-12Co samples at 6 and 9 N, respectively (from final experiments)

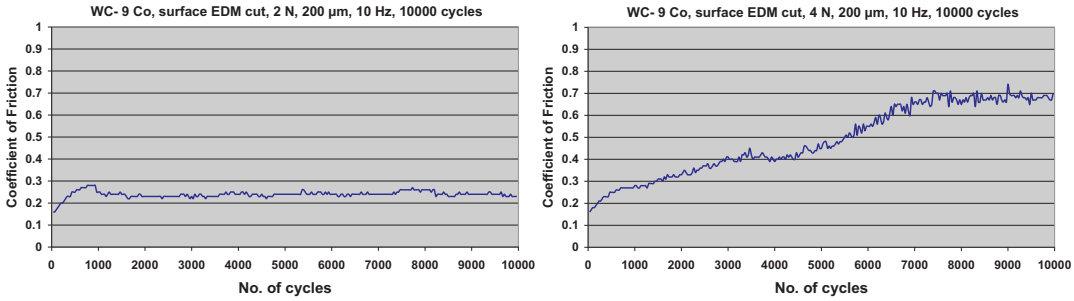

Fig. 6. COF vs No. of Cycles obtained for EDM cut surface of infiltrated WC-9Co samples at 2 and 4 N, respectively (from final experiments)

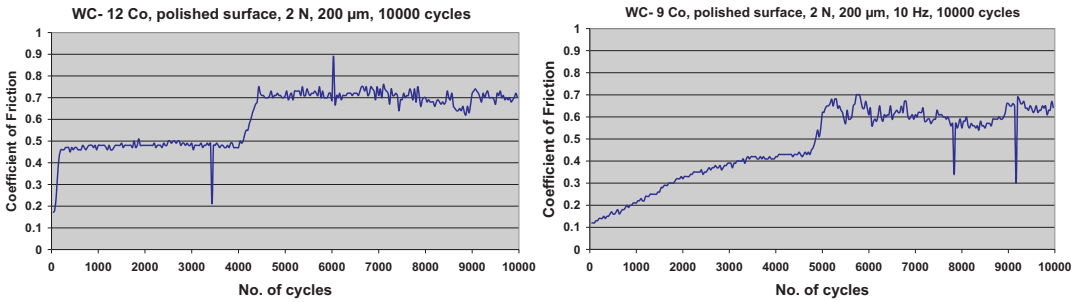

Fig. 7. COF vs No. of Cycles obtained for polished surface of infiltrated WC-12Co and WC-9Co samples at 2 N (from final experiments)

both. At a load of 9 N, WC-12Co depicts a high increase in COF reaching upto 0.55, while in case of WC-9Co an increase occurs already at 4 N. 'Final COF' could be observed by the COF versus No. of cycles graphs for WC-12Co (at loads 6 and 9 N) and WC-9Co (at loads 2 and 4 N) shown in Figures 5 and 6, respectively.

For polished surfaces of both materials, this continuous increase in COF vs. time leading to higher values are observed even at the minimum load of 2 N (see Figure 7). This gives a final COF for WC-12Co and WC-9Co of 0.7 and 0.65 at 2 N load as shown in Table 7.

In order to understand the increase in COF versus time for various samples

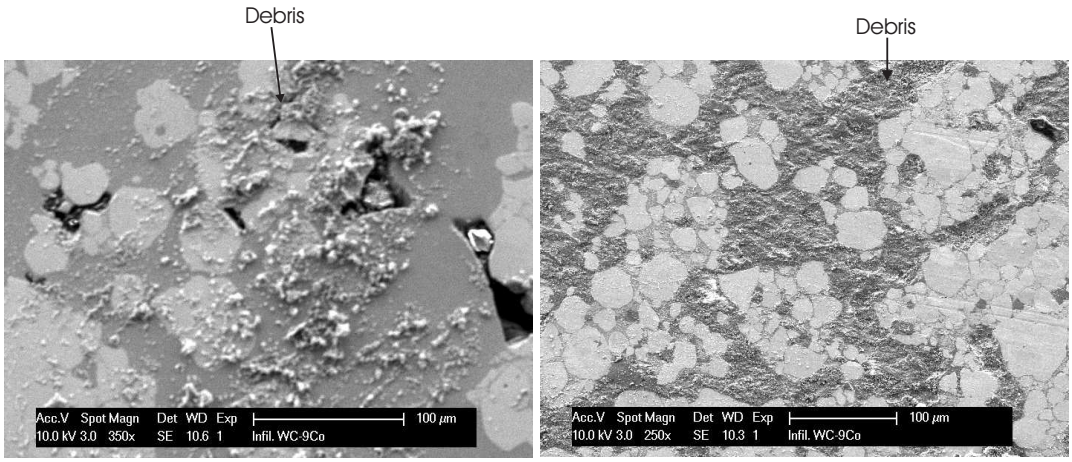

Fig. 8. SEM micrographs of infiltrated WC-9Co samples after fretting tests at 2 and 4 N, respectively (from final experiments)

at various loads, SEM micrographs of wear zones were taken (Figure 8). The micrographs of the WC-9Co polished surface were taken after fretting tests done at loads of 2 and 4 N. The figure shows at both loads of 2 and 4 N, that the sample surface has not been worn out but the chrome steel counterbody has been abraded (see Figure 9) giving rise to debris on the sample (see Figure 8). Figure 9 shows scratch lines on the surface made by friction with the sample.

Continuously wearing out of the counterbody surface has resulted in an increase of friction and consequently an increase in COF. The increase of counterbody wear has been exacerbated by the presence of WC, a hard component. At the EDM cut surface, melting of low melting point component (Co, bronze) has taken place during EDM operation which has prevented the exposition of the hard (WC) phase of the sample to friction with the environment, unlike in case of polished surface. It results in a requirement of higher applied load during wear test for exposing the hard phase to the counterbody in order to increase the COF. Infiltrated WC-12Co has a higher amount of low melting component than that of infiltrated WC-9Co resulting in even higher load of 9 N (for EDMed samples) to be able to observe such increase in COF as shown in 2nd graph of Figure 5.

At a low load of 2 N, the amount of debris is small while at higher load of 4 N, debris has made a thin film as clear from the 2nd micrograph of Figure 8. EDX analysis of the thin film has shown that it is mostly iron originated from the chrome steel counterbody. This has given rise to a change in contact condition in the later stage and friction has taken place not between chrome steel and WC-Co-Bronze but between chrome steel and iron-smeared surface of WC-9Co. The presence of a thin film as shown in the second micrograph of Figure 8 has decreased the final COF of polished WC-9Co surface from 0.65 to 0.4 with an increase in load from 2 to 4 N (see Table 7). In case of EDMed samples, the formation of thin film does not occur even for a fretting

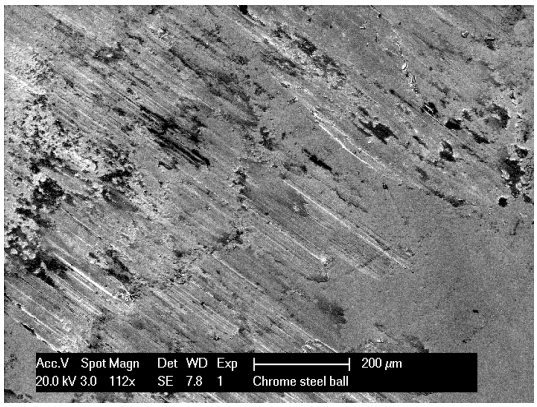

Fig. 9. A SEM micrograph of chrome steel ball after fretting test (from final experiments)

test condition of 9 N load resulting in not a such decrease in COF.

4 Conclusion

The good wear resistance shown by infiltrated WC-9Co is promising and can be used for other wear applications such as cutting tools. Further improvement in the property could be made by the use of smaller WC powders and still higher laser power.

Acknowledgements

The present work is a part of the broader research carried out in the framework of a K. U. Leuven GOA project.

References

[1] S. Vaucher, D. Paraschivescu, C. Andre, and O. Beffort. Selective laser sintering of aluminium-silicon carbide metal matrix composites. *Materials Week*, 2002.

[2] T. Laoui, L. Froyen, and J.-P. Kruth. Effect of mechanical alloying on selective laser sintering of WC-9CO powder. *Powder Metallurgy, vol. 42, No. 3, pp. 203-205*, 2000.

[3] K. Maeda and T. H. C. Childs. Laser sintering (SLS)of hard metal powders for abrasion resistant coatings. *Journal of Materials Processing Technology, vol 149, No. 1-3, pp. 609-615*, 2004.

[4] C. C. Leong, L. Lu, J. Y. H. Fu, and Y. S. Wong. In-situ formation of copper matrix composites by laser sintering. *Materials Science and Engineering A, vol. 338, pp. 81-88*, 2002.

[5] T. B. Sercombe and G. B. Schaffer. On the role of magnesium and nitrogen in the infiltration of aluminium by aluminium for rapid prototyping applications. *Acta Materialia, vol. 52, No. 10, pp. 3019-3025*, 2004.

[6] D. Gu and Y. Shen. WC-Co particulate reinforcing Cu matrix composites produced by direct laser sintering. *Materials Letters, Vol 60, Issue 29-30, pp. 3664-3668*, 2006.

[7] D. Gu, Y. Shen, L. Zhao, J. Xiao, P. Wu, and Y. Zhu. Effect of rare earth oxide addition on microstructures of ultra-fine WC-Co particulate reinforced Cu matrix composites prepared by direct laser sintering. *Materials Science and Engineering:A, vol 445-446, pp. 316-322*, 2007.

[8] D. Gu and Y. Shen. Influencement of reinforcement weight fraction on microstructure and properties of submicron WC-Co_p/Cu bulk MMCs prepared by direct laser sintering . *Journal of Alloys and Compounds, vol 431, No 1-2pp. 112-120*, 2007.

[9] J. Bonse. *A sub-process approach of selective laser sintering.* PhD thesis, K.U.Leuven Faculteit Toegepaste Wetenschappen, 2002.

[10] H. Mohrbacher, J.-P. Celis, and J. R. Roos. Laboratory testing of displacement and load induced fretting. *Tribology International, vol 28, No 5, pp. 269-278*, 1995.

[11] B. Basu, J. Vleugels, and O. Van Der Biest. Microstructure-toughness-wear relationship of tetragonal zirconia ceramics. *Journal of the Europian Ceramic Society, vol. 24 pp. 2031-2040*, 2004.

[12] J. P. Kruth, S. Kumar, and J. Van Vaerenbergh. Study of laser-sinterability of ferro-based powders. *Rapid Prototyping Journal, vol 11, No. 5, pp. 287-292*, 2005.

[13] S. Kumar, J. P. Kruth, and J. Van Humbeeck. Sliding wear behaviour of laser sintered moulds. *2nd International Conference on Polymers and Moulds Innovations, Ghent,Belgium, April 19-20*, 2007.